Correlation between Rheological, Mechanical, and Barrier Properties in New Copolyamide-Based Nanocomposite Films

G. M. Russo,*,† G. P. Simon,‡ and L. Incarnato†

Department of Chemical and Food Engineering, University of Salerno, Via Ponte don Melillo, 84084 Fisciano (SA), Italy, and Department of Materials Engineering, Monash University, Clayton, VIC, Australia 3800

Received October 8, 2005; Revised Manuscript Received March 20, 2006

ABSTRACT: This work focuses on the possibility of improving performance properties of polyamide-layered silicate nanocomposite films for packaging applications by using, as alternative matrix, a statistical copolymer of the nylon-6 having a partially aromatic structure. Nanocomposites at different silicate loadings (commercial organo-modified montmorillonite) were produced by cast-film extrusion using three polyamide matrices: nylon-6 and two copolyamides with similar chemical structure but different molecular weights. Oxygen barrier and mechanical properties of the produced films were investigated and correlated to their nanostructure through analytical techniques sensitive to different aspects of the same morphology, such as TEM, rheological, and dynamic-mechanical analyses. Permeability data were interpolated on the basis of different theoretical approaches, from which a quantitative indication on exfoliation and orientation levels of silicate layers in the matrices was obtained. TEM images at different magnifications were used to empirically evaluate the average length-thickness ratio of silicate platelets and to verify the correspondence with aspect ratios and order parameters calculated by data fitting. A strong correlation between nanomorphology and properties was observed in the different nanocomposite systems and all the three matrices exhibited performance improvement with increasing the silicate content. Nanocomposite films based on the copolyamide with higher molecular weight displayed more exfoliated regions and a preferential orientation of silicate layers, leading to the most significant oxygen barrier improvements and the best mechanical properties.

1. Introduction

The reinforcement of polymers by adding nanoscopic layered silicates is very promising in the production of high-performances plastics.[1−4] The fundamental length scales dominate the morphology of polymer-layered silicate nanocomposites and the uniform dispersion of nanoscopically sized particles can lead a very large interfacial area with bulk properties synergically derived from raw components.

The field of packaging is one for which the application of nanocomposites is highly attractive, and improvements in mechanical and gas barrier properties could allow such materials to be employed as innovative solutions to satisfy the demanding requirements that a modern-day package must fulfill, such as protection, mechanical and thermal resistance, low cost, recycling, etc.[5,6]

Great industrial and scientific attention is paid to polyamide-based nanocomposites prepared by melt compounding either because polyamides are inexpensive, available, and widely used in packaging applications because their hydrophilic nature is the base for a good compatibility with the silicate.[5−10]

The need for higher gas barrier properties of polyamide 6 has been recognized for many years in realizing packaging materials for more sensitive products, and high financial investments have been made to build new monomer and polymer plants to improve gas barrier performances.[11] Among these, the reduction of oxygen permeability is of primary importance, oxygen being one of the principal atmospheric contaminants promoting degradation mechanisms (demolition of organoleptic properties of a food, corrosive phenomena, photooxidations, etc.). The conceptual advantage of polyamide nanocomposites is that interesting performances can be achieved with adding very low filler levels in the matrix. This, coupled with the ability to process such materials on conventional plastics processing equipments, would lead to a net improved performance/cost over the design of new polymers or multilayer materials.

Although significant scientific activity has occurred with regards the use of polyamides as polymer matrices for nanocomposites,[12,13] surprisingly few publications in the literature focus on film extrusion of polyamide nanocomposites, crucial for their technological exploitation.[14,15] The vast majority of all reported nanocomposite research involves injection molding processing, in-situ polymerization techniques, or melt compounding in a mixer, followed by compression molding.[16−18] Moreover, gas barrier properties of polyamide nanocomposite films produced by melt compounding have not been fully investigated and correlated with the degree of dispersion and orientation of silicate platelets inside polymer matrix. The complexity of the final nanostructure makes structure−property relationship not easy to establish and does not allow the observed properties to be explained through conventional composite theories. A significant number of morphological factors, acting on different length scales, affects the achievement of exfoliated silicate structure, and includes the heterogeneity of nanoscale arrangement, the orientational distribution of the anisotropic layers, the strength of polymer−clay interactions, and the conformation and crystallinity of the polymer.[5,15,19,20]

The present work examines the possibility to improve performance properties of nylon-6 nanocomposite films by using a copolyamide matrix, a statistical copolymer of the nylon-6, containing randomly the comonomer 1,1",3-trimethylcyclohexyl-3-methylamine-5-isophthalamide at 5 wt %.

Nanocomposites films at different silicate loadings (3 and 6 wt % of organo-modified montmorillonite) were produced by

† Department of Chemical and Food Engineering, University of Salerno.
‡ Department of Materials Engineering, Monash University.

10.1021/ma052178h CCC: $33.50
Published on Web 05/06/2006

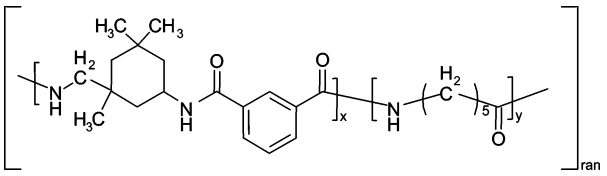

Figure 1. Molecular structure of ADS copolyamide.

Table 1. Melting Temperatures, Intrinsic Viscosity, and Molecular Structure Parameters for the Three Matrices HADS, Nylon 6, and LADS

matrix	traded name	melt T (°C)	intr. viscosity (dL/g)	M_n	M_w
HADS	ADS 40T	212	3.6	53 600	94 420
nylon 6	PA6 FL34	221	3.4	54 200	97 220
LADS	ADS 40T	216	2.9	35 500	62 350

melt compounding using three polyamide matrices: nylon-6 and two copolyamides with similar chemical structure but different molecular weights and viscosities (HADS and LADS). In this way, it was possible to explore the effect of the copolyamide structure and its molecular weight on polymer−clay affinity, nanostructure, and performances.

Our previous studies[21,22] on morphological and rheological characterization of nanocomposite ribbons allowed us to optimize the melt processing conditions (screw speeds in the extruder) to obtain the highest levels of silicate exfoliation.

The aim of this work is to extend the study to the preparation and characterization of corresponding nanocomposite cast films in light of a possible technological application as packaging materials.

In particular the study will focus on the following points:

- analysis of O_2 permeability and mechanical properties and their relationship with the correspondent nanostructure, fundamental in investigating their potential as a packaging film;
- interpolation of permeability data through theoretical models to predict barrier enhancements and obtain a quantitative indication of the state of exfoliation and orientation of the silicate platelets inside the different matrices;
- correlation between O_2 barrier and mechanical enhancements to verify the sensitivity of the different properties to the nanomorphology, and to emphasize the role of polymer matrix on the end performances of nanocomposite films.

2. Experimental Section

2.1. Materials. Three different polyamides supplied by Caffaro SpA (Italy) were used as polymer matrices: nylon-6 and two copolyamides of nylon-6 with low and high molecular weights (denoted LADS and HADS, respectively) having different intrinsic viscosities. The details of the three polymers are shown in Table 1 where it can be seen that the molecular weight of the HADS and nylon-6 are very similar, allowing an interesting comparison of properties. The copolyamide investigated is made by random polymerization of ϵ-caprolactam in the presence of the comonomer 1,1″,3-trimethylcyclohexyl-3-methylamine-5-isophthalamide at 5 wt %; its chemical structure presented in Figure 1.

The silicate used in the preparation of the hybrids was Cloisite 30B (supplied by Southern Clay Products, Inc.), a layered sodium montmorillonite organically modified by methyl, tallow, bis-2-hydroxyethyl, and quaternary ammonium chloride (90 mequiv/100 g clay), having an interlayer basal spacing $d_{001} = 18.5$ Å.

2.2. Melt Processing. The film production was based on two different extrusion stages, as illustrated in Figure 2. In the first, a twin screw extruder, fundamental to required degrees of silicate exfoliation, was used to produce HADS, nylon-6, and LADS nanocomposite pellets containing 6 wt % of the silicate. The extruder was a Haake twin-screw extruder, with a counter-rotating

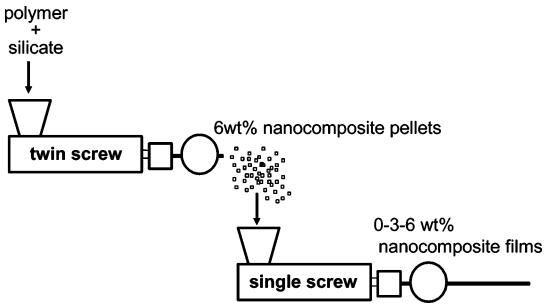

Figure 2. Scheme of processing for the production of HADS, nylon-6, and LADS nanocomposite films at 3 and 6 wt % of silicate content.

Table 2. Average Thickness of HADS, Nylon 6, and LADS Films at Different Silicate Loadings

	film thickness (μm)		
% silicate	HADS	nylon 6	LADS
0	59 ± 5	58 ± 2	61 ± 3
3	65 ± 6	60 ± 4	62 ± 5
6	68 ± 4	68 ± 5	65 ± 6

intermeshing cone-shaped screws, length $L = 300$ mm and, at the end of the extruder, a circular die with a diameter $D = 1$ mm. A screw speed of 100 rpm and a temperature profile of 265−260−255−245 °C from hopper to die were used. Prior to processing, the materials were dried in a vacuum oven at 87 °C for 18 h, resulting in a moisture level of less than 0.2 wt %, to avoid bubble formation and polymer degradation during processing.[23]

Nanocomposite films at 3 and 6 wt % of silicate were obtained by reextruding the 6 wt % nanocomposite pellets with a Gimac single screw extruder of $L = 300$ mm, $L/D = 24$ and a rectangular die with dimensions of 0.25×200 mm^2. The 3 wt % films were obtained by dilution of 6 wt % masterbatch nanocomposite pellets. A screw speed of 100 rpm and a temperature profile identical to the mixing stage were selected. A chill roll rate of 10 m/min was used to collect the films.

2.3. Characterization. The molecular weights (M_n and M_w) of the three neat matrices were determined by GPC analyses at 23 °C by using HFIP/0.05 M potassium trifluoroacetate as eluent and a column with 7 μm particle size. A Shodex Differential refractometer RI71 was used as the detector.

The intrinsic viscosity of the three matrices was determined in H_2SO_4 at 20 °C by using an Ubbelohde viscosimeter.

The final weight percentage of silicate in each of the hybrids was evaluated by drying each sample at 100 °C for 18 h under vacuum and weighting it before placing in a furnace at 900 °C for 45 min in air. The amount of residue was measured and corrected for the loss of organic component present in Cloisite 30B.

The volume fraction of the silicate in each film was determined by density measurements performed on the hybrids and neat materials at 25 °C, with an AccuPyc 1330 densimeter (Micromeritics).

The thickness of the different films was measured through optical microscopy. The average values are reported in Table 2.

Transmission electron microscopy (TEM) analyses were conducted using a Philips EM 208 at different magnification levels. The images were captured on sections normal to the extrusion direction which had been prepared by microtoming of ultrathin specimens with a Leica Utracut UCT microtome.

Rheological measurements in oscillatory mode were performed with a Rheometric Scientific rotational rheometer, ARES (Advanced Scientific Expansion System) in an angular frequency range from 0.1 to 100 rad/s at the temperature of 255 °C using 25 mm diameter parallel plates. The deformation of 1% of strain amplitude was determined from strain sweep measurements in order to ensure linear viscoelasticity of the dynamic tests. Transient stress relaxation measurements in linear regime were taken with a single-step strain of $\gamma_0 = 1\%$ applied at $t = 0$, measuring the shear stress $\sigma(t)$ as a function of time and obtaining the linear stress relaxation modulus

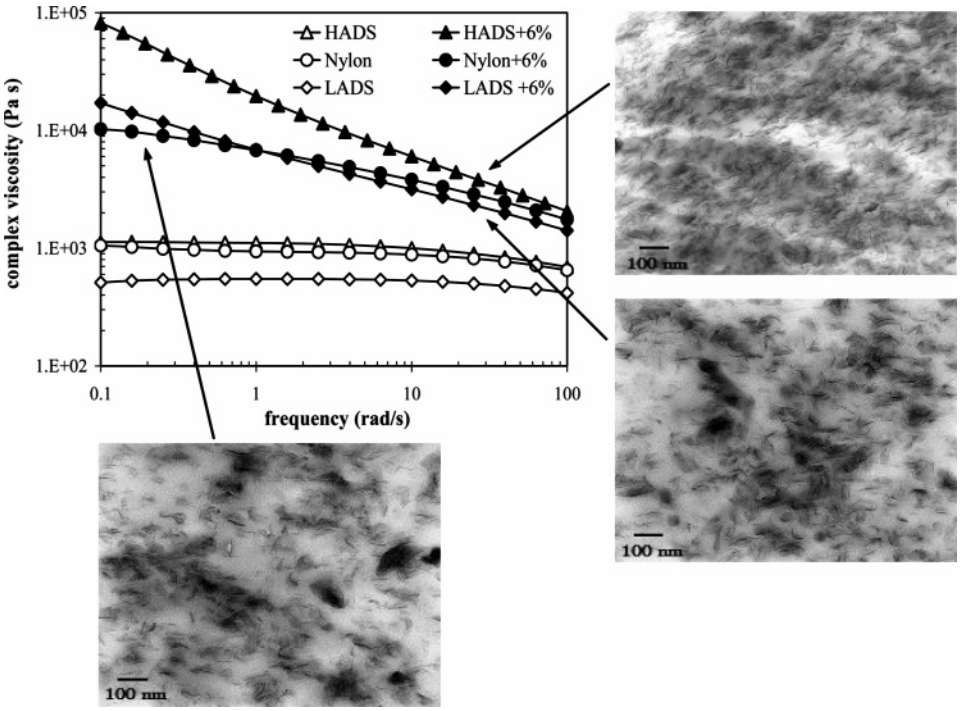

Figure 3. Complex viscosity curves at 255 °C for HADS, nylon-6, and LADS matrices and their respective nanocomposite hybrids at 6 wt % of silicate loading. Micrographs of 6 wt % HADS, nylon-6, and LADS nanocomposites are related to the appropriate curves.

$G(t)$ as $G(t) = \sigma(t)/\gamma_0$. All rheological experiments were conduced under a nitrogen atmosphere to prevent oxidative degradation of the specimens, and prior to the tests, the samples were dried for 16 h in a vacuum at 85 °C.

Oxygen permeability of the films was determined with GPC-D Brugger permeability device at 30 °C according ASTM D1434 procedure. The equipment consists of two chambers between which the film is placed. The chamber upon the film is filled of oxygen with the pressure of 1 atm. A pressure transducer, set in the chamber below the film, records the increasing of O_2 pressure, P, as a function of the time, t. From pressure−time plot, the software automatically calculates permeation, that can be converted in permeability known the film thickness. The diffusion coefficient, D, was calculated through the equation[34]

$$D = l^2/6\tau \quad (1)$$

where l is the thickness of the film and τ is time lag, evaluated from pressure−time plot provided by the software.

Thermal behavior of the films was determined using a Mettler differential scanning calorimeter (DSC30), and performing the following thermal cycle: a first heating at 10 °C/min from 0 to 260 °C; an isotherm at 260 °C for 10 min to melt the residual crystals and remove the thermomechanical history; a cooling to 0 °C and a reheating to 260 °C at the same scan rate. Crystallinity degrees, X_c, of the different films were determined by the ratio of heat of fusion of the sample on heat of fusion of the purely crystalline nylon-6, i.e., 240 J/g.[33]

X-ray analyses were performed with Philips 1130 diffractometer, using Ni-filtered Cu Kα radiation and analyzing the angles from 1 to 30° at a scan rate of 2°/min.

Dynamic-mechanical analyses were carried out in the tensile mode using a DMTA IV (Rheometric Scientific) with a strain of 0.03%, a frequency of 1 Hz, and a heating rate of 2 °C/min in the range of 10−180 °C.

Mechanical tests in tensile mode were performed with a Dynamometer (Instron 5566) in a conditioned room at 23 °C and 50% HR, imposing a cross speed of 50 mm/min and cutting the films with a rectangular geometry of 12.7 × 80 mm^2, according to the ASTM D-638 procedure.

3. Results and Discussion

Our previous studies[21,22] on morphological and rheological characterization of nylon-6 and LADS nanocomposite ribbons (thickness about 3 mm) had allowed us to analyze the effects of the copolyamide matrix and melt processing conditions (extrusion rates) on dispersion and distribution of silicate platelets inside the polymer matrices. The most significant results suggested stronger polymer−clay interactions in the presence of the copolyamide matrix.

In the present work, the study is extended to the preparation and characterization of corresponding nanocomposite cast films (thickness about 60 μm) as packaging materials.

Moreover a copolyamide (HADS) with the same chemical structure of LADS and molecular weight similar to nylon-6, was used for the preparation of nanocomposite films, allowing interesting comparison of properties with the homopolymer based hybrids.

HADS, nylon-6, and LADS nanocomposites at 3 and 6 wt % of silicate loadings were produced through a cast film processing described in the Experimental Section. The properties of the three polymers are outlined in Table 1.

The film production was based on two extrusions stages, illustrated in Figure 2. The use of a twin screw extruder in the first stage is fundamental in realizing an homogeneous dispersion and high levels of silicate exfoliation.[12] The mixing conditions were selected on the basis of our previous works.[21,22]

The amount of silicate exfoliation achieved in HADS, nylon-6, and LADS nanocomposites inside the twin extruder was verified through rheological and TEM investigations. As demonstrated from the literature,[1,22,24−26] rheological behavior is strongly correlated to degree of exfoliation and intercalation of the silicate platelets in the polymer matrix.

Figure 3 shows the plot of complex viscosity (η^*) vs angular frequency (ω) for the pure matrices, HADS, nylon-6, and LADS, and their respective nanocomposites pellets containing 6% organoclay. It should be noted that despite chemical differences between neat HADS and nylon-6, the similarity of intrinsic

viscosities and molecular weight translates into comparable melt viscosity values, while the lower molecular weight LADS matrix displays a lower complex viscosity. Comparing the rheological curves of HADS and nylon-6 nanocomposites, it can be seen that the HADS-based hybrid shows a higher complex viscosity and stronger incremental increases of η^*, with respect to virgin polymer. Moreover, it exhibits a frequency dependence in all the range of frequencies investigated. Analyzing the corresponding TEM images, shown in Figure 3, a significant difference in morphology in the two hybrids can be seen. In particular, the HADS system whose complex viscosity is markedly shear thinning, exhibits a more uniform dispersion of clay particles and a higher degree of silicate exfoliation with a preferential orientation of the layers. Since the intrinsic and melt viscosities of HADS and nylon-6 matrices are comparable, the different rheological behavior and nanostructure in the respective hybrids can be attributed to better polymer−silicate interactions present in HADS-based system.

The influence of the molecular weight (and thus viscosity) of the copolyamide matrix on the rheological behavior of the respective hybrids can be evaluated by comparing the viscosity curve of nanocomposite based on HADS with that based on LADS (Figure 3). HADS hybrid displays higher values of complex viscosity and a more pronounced "shear thinning" behavior. The difference may be attributed to the higher melt viscosity of HADS matrix that produces greater shear stresses on the silicate stacks during mixing in the extruder, according to reports on the effect of molecular weight of polyamide matrix in nanocomposite systems.[12,25] This leads to a greater reduction in silicate stack dimensions, promoting a more homogeneous and uniform dispersion of silicate platelets, as observed by the corresponding TEM images in Figure 3. It is interesting to observe that the 6 wt % LADS based nanocomposite shows nanostructure and rheological behavior comparable to nylon-6 hybrid, despite its lower viscosity and thus reduced shear stress during blending.

All of these outcomes suggest that the better silicate dispersion in HADS matrix, compared with the two other matrices, can be related to more favorable polymer chain ingress inside silicate interlayers. This can be principally due to the affinity with the clay with the presence of comonomer in nylon-6 and also to higher molecular weight that promotes higher shear stresses which favor silicate delamination.

However, it should also be noted that in all the nanocomposite samples, the distance between well-exfoliated platelets is itself of a nanosized scale. As example, it can be seen from the TEM images in Figure 3 that the average distance between layers is of the order of 10−50 nm. In comparison, the distance between the entanglements can be calculated using semiempirical equations and summing of second neighbor backbone atoms. Given that the molecular weight between entanglements for nylon-6 is 2084 g/mol,[27] the contour length can be determined by summing the distance between second neighbor backbone atoms. Since the C−C bond length is 0.154 nm, while the C−C−C second neighbor distance is 0.255 nm, in a fully extended $(CH_2)_5$−CONH− monomer group the length is 0.9 nm. This monomer amounts to 113 g/mol, so the entanglement distance for nylon-6 corresponds to 0.9 nm × 2084/113 = 16.6 nm. Thus, spacing between clay layers in the melt is indeed of a comparable size to the entanglement length of the nylon (some two to three times the entanglement distance), which means that the dynamic network of the polymer chains is likely to be strongly perturbed when there is a full-scale delamination of platelets.

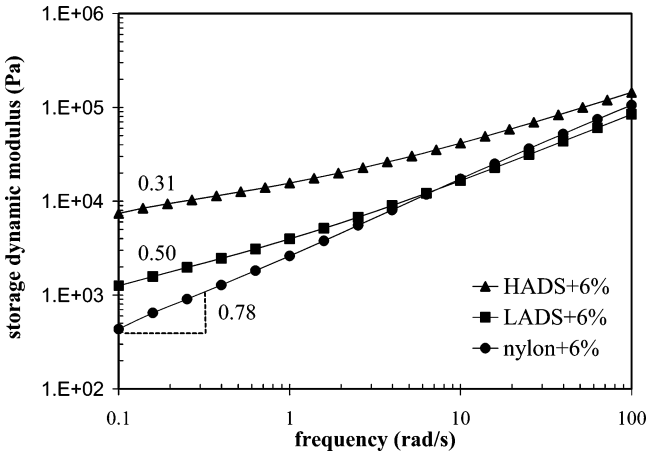

Figure 4. Storage modulus plots at 255 °C for the 6 wt % nanocomposite pellets, based on the three different matrices: HADS, nylon-6, and LADS. The slope at the low frequence is also reported for the three systems.

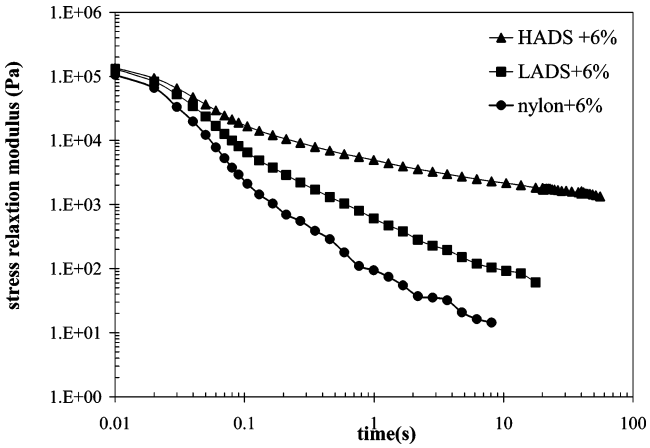

Figure 5. Linear stress relaxation modulus $G(t)$ at 255 °C of 6 wt % nanocomposite pellets, based on the three different matrices: HADS, nylon-6, and LADS.

The structural network formed in the three different nanocomposites greatly influences the storage modulus (G'), as it is very sensitive to morphological state. A comparison of the G' values of HADS, nylon-6, and LADS pellets with the 6 wt % of silicate, is shown in Figure 4. In agreement with the complex viscosity, HADS based nanocomposite shows the highest G' values and a more pronounced pseudo-solid behavior. This can be seen from the lowest G' slope at low angular frequencies that is 0.31 for HADS hybrid and 0.78 and 0.50 for nylon-6 and LADS hybrids, respectively.

The relaxation of the three hybrids was further analyzed through the transient stress relaxation measurements, being dynamic oscillatory moduli G' and G'', both related to linear stress relaxation.[28]

In Figure 5, stress relaxation moduli $G(t)$ vs time for the three different 6% nanocomposite systems are reported. The graph clearly shows that HADS hybrid retains the greatest values of stress relaxation modulus at long times. Both the dynamic oscillatory and stress relaxation moduli represent a further confirmation of the higher clay dispersion and exfoliation levels with stronger polymer−silicate interactions in HADS nanocomposites.[5,22]

Following the achievement of satisfactory silicate exfoliation in the three different 6% nanocomposite pellets, films of

Table 3. Oxygen Permeability Values (*P*) and Crystallinity Degrees (X_c) of HADS, Nylon 6, and LADS Based Nanocomposites Films at Different Silicate Loadings[a]

	HADS films		nylon 6 films		LADS films	
silicate content (%)	*P*	X_c (%)	*P*	X_c (%)	*P*	X_c (%)
0	0.207	24	0.189	30	0.184	26
3	0.138	26	0.163	29	0.172	25
6	0.095	26	0.137	31	0.149	25

[a] Measured units of permeability values are cm^3 cm/(m^2 day bar).

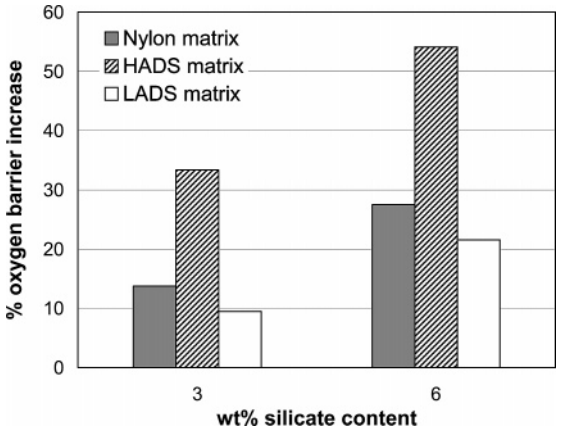

Figure 6. Percentage increments of O_2 barrier properties in HADS, nylon-6, and LADS nanocomposite films.

exfoliated systems were produced using a cast film process, described in the Experimental Section. A range of properties of the films were investigated, an important one being oxygen permeability, since barrier properties are key for packaging films. However, we were particularly interested to determine the degree to which barrier properties are a sensitive indicator to the degree of silicate dispersion.

Table 3 reports permeability values (*P*) and crystallinity degrees (X_c) of HADS, nylon-6, and LADS nanocomposite films at different silicate contents. All the three matrices show a decrease in oxygen permeability with increasing of silicate loading. In particular, for any fixed silicate loading, HADS-based films always exhibit the lowest permeability values even if they are characterized by low crystalline contents, while the permeability values of LADS nanocomposite and nylon-6 films are comparable, according to the morphological and rheological results. For instance, it can be seen that the 6 wt % HADS hybrid permeability (0.095 cm^3 cm/(m^2 day bar)) is even 31% lower than the corresponding nylon-6 hybrid (0.137 cm^3 cm/(m^2 day bar)) and 36% lower than the 6 wt % LADS (0.149 cm^3 cm/(m^2 day bar)), giving the HADS matrix interesting O_2 barrier properties when combined with silicate.

Moreover, it is possible to observe that the presence of silicate in HADS matrix has a greater effect on permeability reduction compared with other matrices: the addition of 6 wt % of silicate in HADS matrix causes a decrease in permeability of about 54%, while the same quantity of silicate leads to a decrease of 28% in the nylon-6 permeability and of 21% in the LADS permeability. Figure 6 shows O_2 barrier increases for the three systems analyzed at different weight percent silicate contents.

To better understand the observed reductions of permeability and the role of the chemical structure of the copolyamide matrix, we have to take into account the principal factors affecting permeability related both to polymer and silicate, such as degree of crystallinity and crystal phases of the polymer, mobility of amorphous phase, levels of dispersion and orientation of silicate platelets inside the matrix.

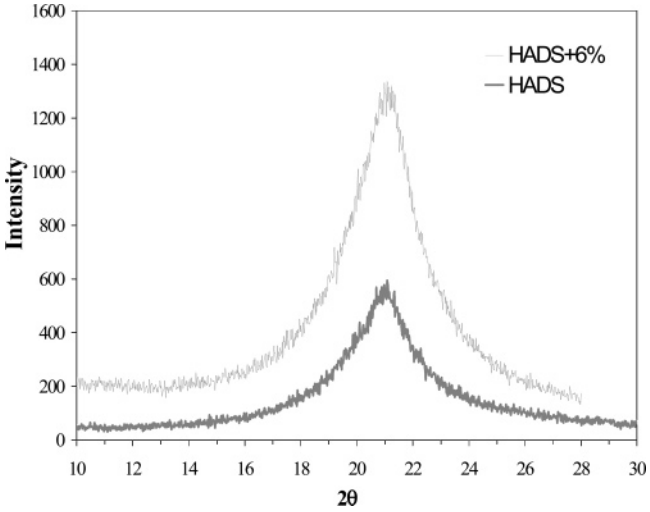

Figure 7. X-ray profiles of neat HADS matrix and its 6 wt % silicate nanocomposite film.

It is known that the addition of layered silicate can change the degree of crystallinity, most often acting as a nucleant, as well as causing different crystal structures.[29,30] Polyamides can, in fact, display two principal crystal forms: the α-phase, thermodynamically the most stable, and the γ-phase, obtained under nonisothermal crystallization conditions, particularly for rapid cooling such as at the surface of injection molded samples.[21,29−31]

As shown in Table 3, the addition of silicate in the three matrices HADS, nylon-6, and LADS does not cause significant variations of crystallinity degree.

With regards to the crystalline structure, all films were characterized only by the γ crystal form. As example, Figure 7, comparing X-ray spectra of neat HADS and its 6% hybrid film, clearly shows the presence of only a peak centered at 21.2°, related to the γ crystal phase. Similar patterns were obtained for all the other samples. Kyotani and Mitsuhashi have shown that the rate of γ-formation is faster than α-formation at lowest cooling temperatures.[32] The low thickness of the films (50−70 μm) could thus cause very fast cooling at the exit of the extruder, promoting the γ-phase. This would be in agreement with the results of Fornes and Paul who demonstrate the presence of the only γ-phase in the skin of nylon nanocomposite samples from injection molding, and both α−γ phases in the core.[33]

Dynamic mechanical analyses (DMA) were performed on HADS and nylon-6 films in the solid state in order to determine their relaxational properties and investigate how the presence of silicate layers alters the conformation and mobility of the two different matrices.

DMA represents a good method of correlating the performance of the films with the presence of more or less constrained regions. This is of particular interest with regards gas permeability, since it is highly sensitive to the mobility of amorphous phase.

In parts a and b of Figure 8, the storage moduli *E′* of the neat matrix and the 6 wt % hybrid are compared for HADS and nylon-6-based nanocomposite films. Analyzing the curves, it can be seen that the moduli *E′* of both 6% nanocomposite films are always greater than their own neat matrices over all temperatures investigated, and the drop in values of *E′* is always lower than for the virgin polymers. In particular, 6 wt % HADS hybrid displays, at any temperature,

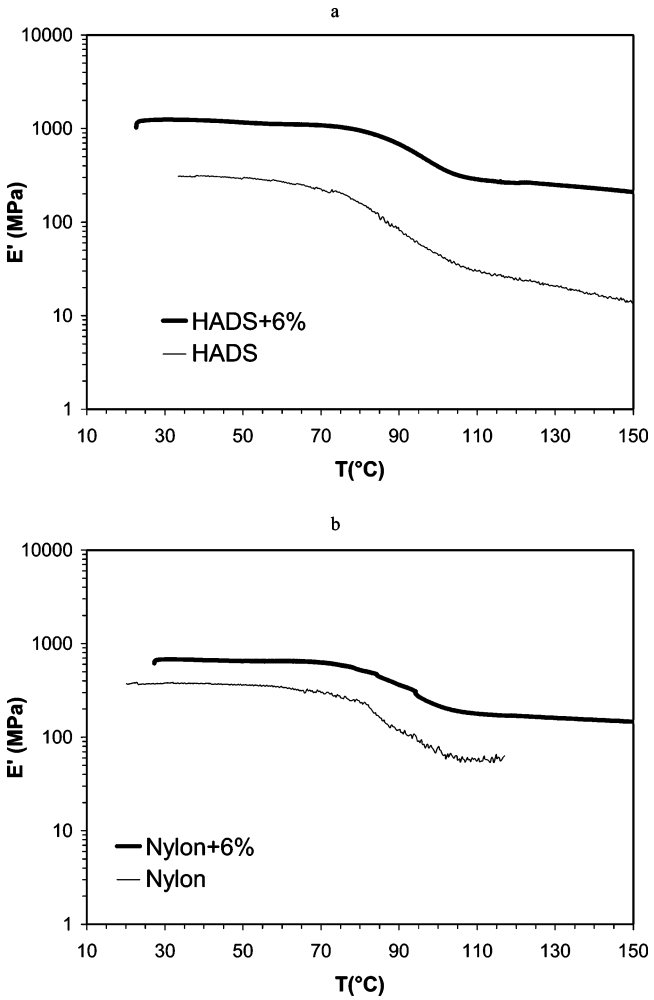

Figure 8. Storage modulus as a function of temperature: (a) HADS and HADS+6 wt % silicate films; (b) nylon-6 and nylon-6+6 wt % silicate films.

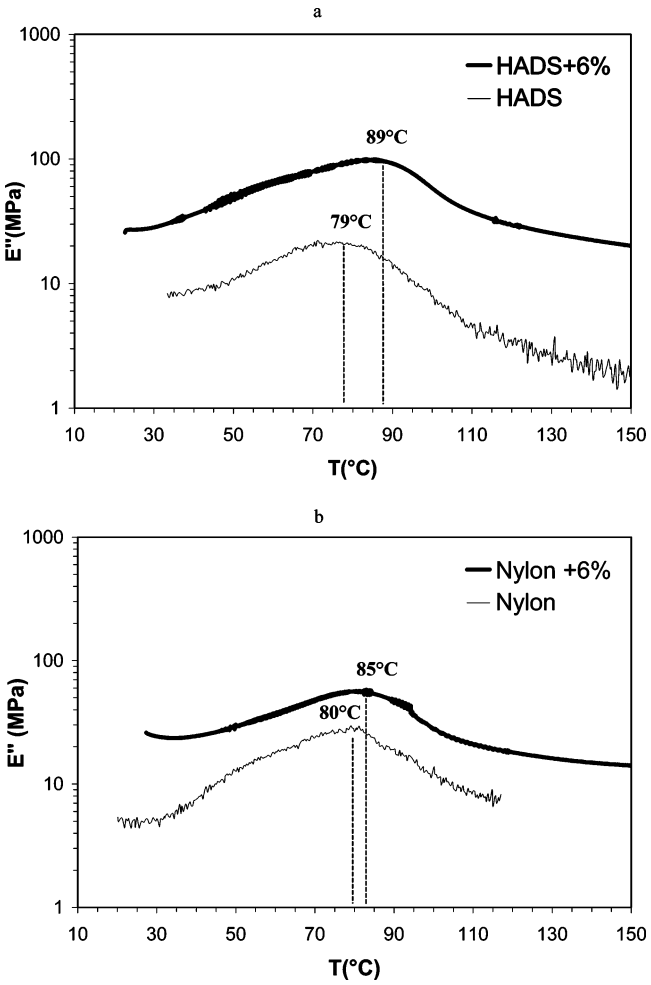

Figure 9. Loss modulus as a function of temperature: (a) HADS and HADS+6 wt % silicate films; (b) nylon-6 and nylon-6+6 wt % silicate films.

higher E' values and stronger increments with respect to its own matrix when compared with the correspondent nylon-6-based nanocomposite. As an example, the ratio between nanocomposite/matrix moduli is about 4 and 2 at 35 °C and 10 and 3 at 115 °C for HADS and nylon-6 films, respectively.

Differences between HADS and nylon-6-based films are also shown by the behavior of the dynamic loss modulus E'', reported in Figure 9a,b. A shift in the glass−rubber transition from 79 to 89 °C was found in the HADS hybrid with respect to the neat matrix, while a slightly lower shift from 80 to 85 °C was observed in the nylon-6 system.

Nanocomposite DMA results can be attributed to the confinement of amorphous polymer chains in silicate galleries that partially hinders the molecular motions. This effect is more evident in HADS nanocomposites, indicating a reduced mobility of amorphous phase in such a system.

Gas permeation is greatly dependent by the diffusion process of the gas through the polymer.[34] The presence of silicate in nanocomposite films can make more tortuous the diffusive path for the permeant gas. Therefore, O_2 diffusion coefficients (D) can be strongly affected by the nanomorphology achieved in the samples. In this regard, D values of the different films were evaluated according to the procedure described in the Experimental Section.

Figure 10 shows the dependence of D on clay content in HADS, nylon-6, and LADS films. Comparing the results, it is clear that HADS hybrids are characterized by stronger decreases in D values, suggesting a more tortuous path of the gas during its transport through polymer.[14,35] This can be related to a better dispersion of the silicate inside copolyamide matrix that hinders the path of O_2 molecules.

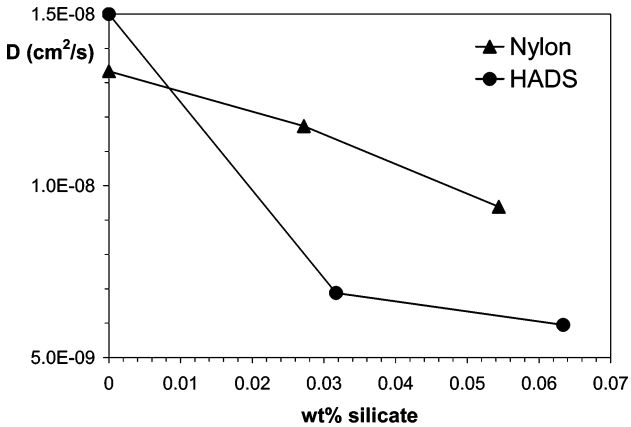

Figure 10. Dependence of diffusion coefficient, D, on clay content in HADS and nylon-6 films.

To quantify the levels of silicate exfoliation in two different matrices HADS and nylon-6 the permeability data were interpolated on the basis of the Nielsen theory,[35] expressed by the following equation:

$$\frac{P}{P_m} = \frac{1-\phi_f}{1+\frac{\alpha}{2}\phi_f} \tag{2}$$

where P and P_m are respectively the permeability of the nanocomposite and the pure matrix, ϕ_f is the volume fraction of the filler, and α is its aspect ratio.

In this simple model, based on the longer diffusive path that a gas must travel in the presence of a filler, the reduction of permeability depends on the quantity of the filler and its aspect ratio. This means that, at fixed types and loading of silicate, the best gas barrier properties of a nanocomposite hybrid can be achieved by maximizing the aspect ratio, the structural parameter present in eq 2. Since the clay intrinsically has particles with a range of aspect ratios due to heterogeneity of arrangement on the nano and microscale, this parameter can be thought to be an average aspect ratio whose value is indicative of the degree of dispersion.

Applying eq 2 to the experimental data, α was determined from the best fit. Figure 11 shows the α values calculated from eq 2 fitting, which are 57 and 20, respectively, for HADS and nylon-6 films. The calculated value of aspect ratio in HADS hybrid, is more than double that of nylon-6-based films and indicates a better nanoscopic dispersion of the silicate inside the copolyamide matrix. This was confirmed by further TEM analysis performed on 6 wt % HADS and nylon-6 nanocomposite films, whose images are shown in Figure 12a,b. A similar intercalated/exfoliated nanostructure characterizes both the systems, but a more uniform distribution of silicate platelets with smaller sized silicate aggregates can be observed for the HADS based hybrid, in agreement with the calculated aspect ratios.

TEM images at different magnifications were used to empirically evaluate the average length-thickness ratio of silicate platelets-stacks and to compare with the aspect ratios based on the Nielsen model. Parts a and b of Figure 13 show an example of graphical determination of aspect ratio from HADS+6% TEM image.

The average aspect ratios obtained with the graphical approach were 76 and 48, respectively, for HADS and nylon-6 nanocomposite films, higher than the values calculated by the Nielsen fit. Although of broadly the same size scale and relative magnitudes, the theoretical values (from the model fitting) were less than those determined by experiment (TEM). This disparity can be explained in a number of ways. First, TEM images show small regions of nanocomposite sample and for this they are not representative of the global nanostructure. Moreover, the Nielsen model considers a full exfoliation of the total amount of silicate present in each composite; therefore only a lower volume fraction, corresponding to the well-exfoliated silicate fraction, should be considered in the Nielsen fitting. In addition, we have to take into account the simplicity of the Nielsen model in which many structural factors are not considered, such as the relative orientation of the layers in the matrix, the sheet lengths, and the state of aggregation and dispersion of the silicate. The model proposed by Nielsen, for example, supposes that each layer is oriented perpendicularly to the direction of diffusion of the gas, leading to the most tortuous path for the permeant. The micrographs indicate instead that the platelets are generally not oriented in this fashion but are more random. Thus, the full planar nature of the layered silicates and its maximum ability to hinder gas transmission is not realized and the effective value of α is less than that measured directly by TEM.

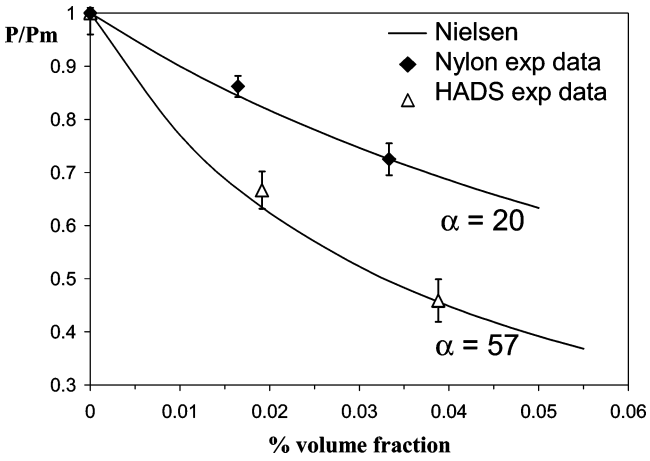

Figure 11. Experimental permeability data against silicate volume fraction fitted by Nielsen theoretical equation to obtain the best fitting average values of aspect ratio α.

On the basis of these considerations, Bharadwaj[14] modified the simple model of Nielsen by including in the equation the order parameter, S, of the layers through the following equation

$$\frac{P}{P_m} = \frac{1-\phi_f}{1+\frac{\alpha}{2}\phi_f\left(\frac{2}{3}\right)\left(S+\frac{1}{2}\right)}$$

with

$$S = \frac{1}{2}(3\cos^2\vartheta - 1) \tag{3}$$

where S is the order parameter and ϑ is the angle between the direction of gas flow and the normal of the layers, as illustrated in Figure 14. In this way, all the possible arrangements of the silicate layers in the polymer matrix can be accommodated. When $S = 1$ the layers are perfectly oriented perpendicular to the direction of gas flow (expression reduces to Nielsen), when $S = 0$ the layers are randomly oriented without a preferential direction and when $S = -1/2$ layers are oriented parallel to the direction of gas flow so that the permeability of the hybrids coincides with the neat polymer.

Equation 3 can give an indication on the state of orientation of the silicate layers inside the polymer matrix, if the aspect ratio of a nanocomposite system is known. Introducing into eq 3 the values of aspect ratio obtained by graphical analysis of TEM images, it was possible calculate, from best fits, the values of the order parameters, S, in the two systems. Figure 15 shows the fitting of permeability data with the eq 3, leading to S values of 0.55 and 0.15 respectively for HADS and nylon-6 based films, far from the condition of $S = 1$ assumed by Nielsen theory.

Table 4 summarizes the values of aspect ratio obtained with the different approaches previously described. All suggest a higher fraction of well-exfoliated silicate platelets in HADS films. The higher S value found for HADS films confirms the more pronounced orientation of the silicate platelets layers in HADS matrix, as observed from TEM images in Figure 12a,b.

On the basis of such results, the observed enhancements of gas barrier seem not related to variation of crystallinity degree or crystal phases but to polymer−clay interactions affecting the mobility of amorphous phase and the levels of dispersion and orientation of silicate platelets inside the matrix.

The mechanical properties in tensile mode of nanocomposite films were investigated in order to complete the analysis of film behavior.

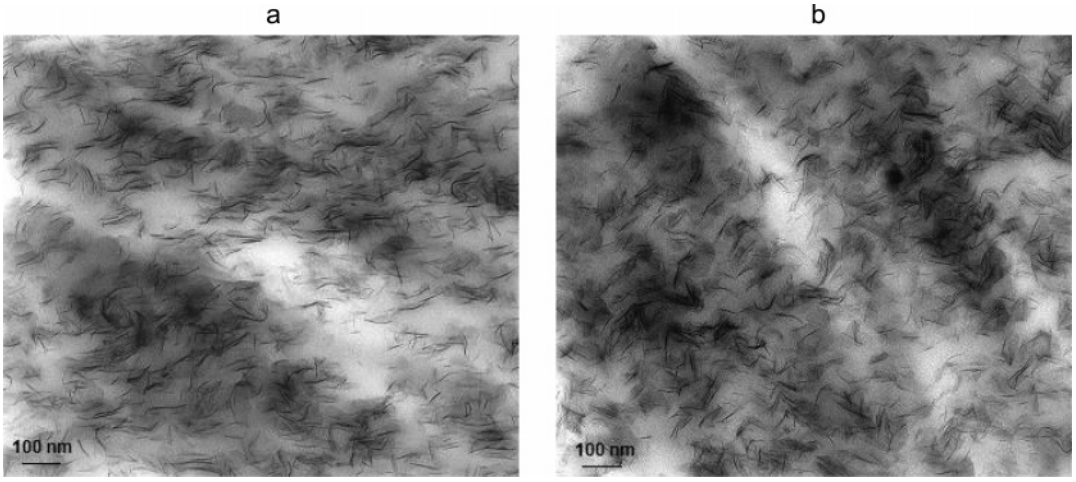

Figure 12. TEM images of 6 wt % silicate nanocomposite films: (a) HADS matrix; (b) nylon-6 matrix.

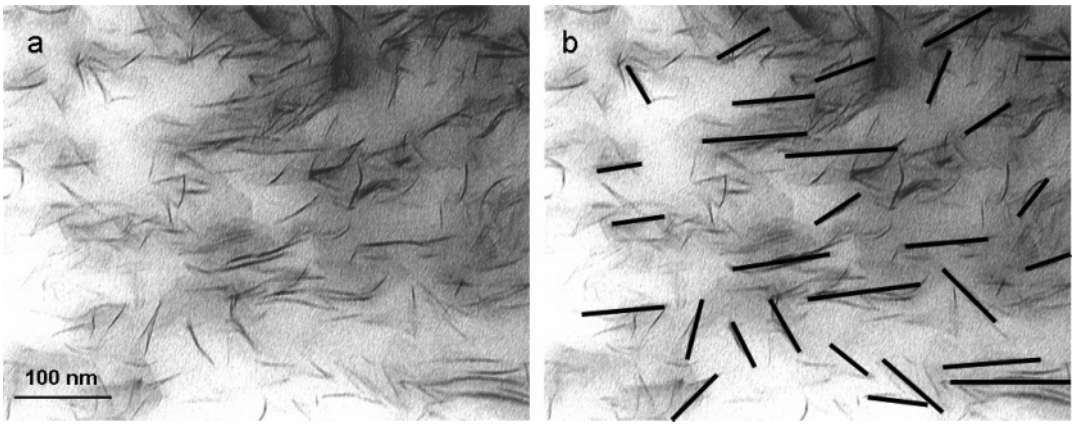

Figure 13. Example of calculation of the average aspect ratio from HADS +6 wt % silicate nanocomposite TEM images: (a) image before the calculation; (b) same image after the calculation.

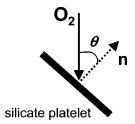

Figure 14. Orientation of the silicate with respect to the direction of oxygen flow. θ is the angle between the normal at silicate plane and the direction of oxygen.

Table 5 reports tensile modulus (E), ratio's of nanocomposite modulus to neat polymer, yield stress, stress at break (σ_b), and elongation at break (ϵ_b) of HADS, nylon-6, and LADS films.

The presence of silicate leads to substantial improvements in stiffness (tensile modulus) and yield stress in all the three matrices. In particular, HADS-based hybrids exhibit the highest relative modulii for all silicate concentrations, while LADS films display modulus values similar to the correspondent nylon-6 films, in agreement with both rheological and gas barrier behaviors.

A reduction of the elongation at break, more pronounced in nylon-6 films, is also shown by nanocomposites systems with respect to their own matrices, likely associated with the increased stiffness of the hybrids.

It should be noted that most studies on mechanical properties of nylon-6 nanocomposites (usually injection molded specimens) show a brittle fracture in the hybrids with elongations at break around 6−60%, usually ascribed to the presence of unexfoliated aggregates creating discontinuities in stress transfer between the two chemically different phases.[13,15] The films produced in this work retain instead higher levels of ductility, likely due to the good dispersion of clay within the matrix and to the presence of few, bulky tactoids.

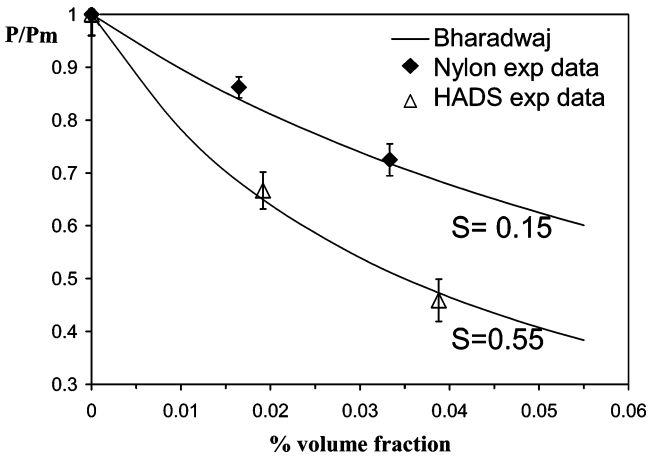

Figure 15. Experimental permeability data against silicate volume fraction fitted by Bharadwaj theoretical equation (eq 3). The order parameters, S, were obtained from the best fitting by introducing in the equation the α values estimated from TEM images, that are 76 and 48, respectively, for HADS and nylon-6 nanocomposite hybrids.

Moreover, decreases in the stress at break are shown by nylon-6 and LADS matrices as increasing silicate loading, with lower reductions in copolyamide hybrids. Conversely, the presence of silicate in HADS matrix leads to significant increases of stress at break, even if HADS is the matrix with the lowest stress at break. Such behavior is a further indication of good adhesion between polymer and clay that facilitates

Table 4. Aspect Ratios Values, α, Calculated for HADS and Nylon 6 Films through Three Different Approaches: Nielsen Fitting (eq 2); Graphical Evaluation from TEM Images; Eq 3 Fitting[a]

polyamide matrix	Nielsen fitting (eq 2)	graphical evaluation (TEM)	Bharadwaj fitting (eq 3)
HADS	$\alpha = 57$	$\alpha = 76$	$\alpha = 76$; $S = 0.55$
nylon 6	$\alpha = 20$	$\alpha = 48$	$\alpha = 48$; $S = 0.15$

[a] In the third case, the order parameters, *S*, are calculated by using α values from graphical evaluation.

Table 5. Tensile Modulus (E), Relative Modulus (E/E_m), Yield Stress (σ_Y), Stress at Break (σ_b), and Elongation at Break (ϵ_b) for HADS, Nylon 6, and LADS Nanocomposite Films with Different Silicate Loadings

film composition (%)	E (MPa)	relative modulus	σ_Y (MPa)	σ_b (MPa)	ϵ_b (%)
		HADS			
0	1380 ± 30	1	38 ± 2	56 ± 2	330 ± 40
3	1960 ± 90	1.42	40 ± 3	60 ± 3	280 ± 10
6	2480 ± 70	1.80	51 ± 3	66 ± 5	240 ± 10
		Nylon 6			
0	1260 ± 80	1	36 ± 3	73 ± 3	350 ± 20
3	1670 ± 60	1.32	37 ± 2	58 ± 2	220 ± 30
6	2000 ± 20	1.59	40 ± 2	50 ± 7	180 ± 40
		LADS			
0	1310 ± 80	1	34 ± 4	67 ± 3	360 ± 30
3	1700 ± 30	1.30	36 ± 3	58 ± 3	300 ± 30
6	1950 ± 30	1.49	41 ± 3	50 ± 5	260 ± 20

the stress transfer to the reinforcement phase, and translates to better mechanical properties.

Given the seemingly good qualitative correlation between TEM, gas barrier and mechanical properties for the different systems, a comparison of the ratio of nanocomposite/matrix permeability to the ratio of nanocomposite/matrix tensile modulus is shown in Figure 16. The graph clearly shows a monotonic dependency of the two parameters, suggesting that their values arise from the same source: the degree of dispersion and delamination of the layered silicates within the polymer. The lower-lying value of the HADS line correlating gas barrier with mechanical properties indicates that the inclusion of the comonomer in nylon-6 to form the ADS copolymer chains leads to better enhancements of the end performances, derived from a more effective silicate dispersion in the matrix for any silicate loading that, in turn, can be associated with stronger polymer−silicate interactions.

4. Conclusions

In this work nanocomposite films at different silicate loadings (3 and 6 wt % of organo-modified montmorillonite) were produced by cast film extrusion using three polyamide matrices: nylon-6 and two copolyamides with similar chemical structure but different molecular weights (HADS and LADS). Oxygen barrier and mechanical properties were investigated and related to their nanomorphology through TEM microscopy, rheological, and dynamical mechanical analyses.

All the three matrices showed improvements of O_2 barrier and mechanical properties as increasing the silicate content. In particular, nanocomposite films based on copolyamide with higher molecular weight (HADS) exhibited the best end performances. The observed enhancements of properties seemed to be unrelated to variation of crystallinity degree or crystal phases but related to dispersion and orientation of silicate platelets inside the matrix, as well as to the possible presence of polymer−clay interactions.

Permeability data were interpolated on the basis of different theoretical approaches, from which a quantitative indication on exfoliation and orientation levels of silicate layers in the different matrices was obtained. The aspect ratios and order parameters calculated by data fitting were compared with those empirically evaluated from TEM images, and suggested higher fractions of well exfoliated silicate platelets and a more pronounced orientation of the layers inside the HADS copolyamide matrix.

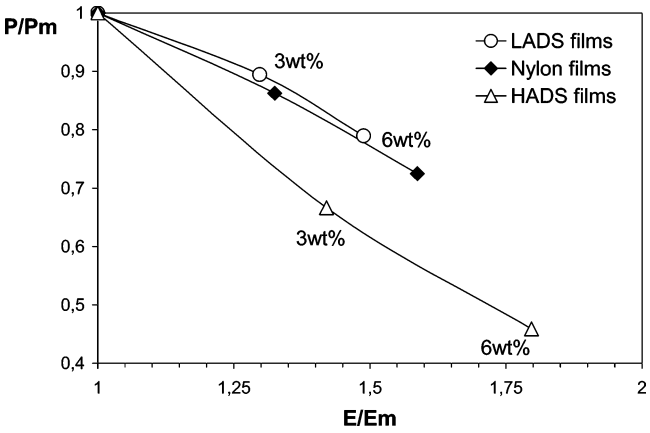

Figure 16. Nanocomposite/matrix permeability ratio as a function of nanocomposite/matrix tensile modulus ratio for HADS, nylon-6, and LADS films at different silicate loadings.

The better nanomorphology in HADS hybrids was confirmed by the strongest decreases of O_2 diffusion coefficients, leading to a more tortuous path of O_2 molecules during their transport through the polymer. The good affinity of HADS matrix with the silicate was seen by slower relaxation of polymer chains (pseudo-solid like behavior) and a reduced mobility of the amorphous phase as shown by rheological and DMA analyses.

Moreover, HADS hybrids were the only samples to show enhancement of stress at break with the silicate loading, suggesting good adhesion between organic and inorganic phases.

The qualitative correlation between tensile modulus and O_2 permeability of the three systems, in strong agreement with rheological and morphological features, clearly showed the best performances of the HADS nanocomposite films, principally due to the affinity of HADS with the clay for the presence of comonomer into nylon-6 structure. Higher molecular weights that promote higher shear stresses which favor silicate delamination are also of importance.

Acknowledgment. Thanks to Dr. Alfred Uhlherr of CSIRO for calculations relating to entanglement distance.

References and Notes

(1) Giannelis, E. P.; Krishnamoorti, R.; Manias, E. *Adv. Polym. Sci.* **1999**, *138*, 107.
(2) Ke, Y.; Long, C.; Qi, Z. *J. Appl. Polym. Sci.* **1999**, *71*, 1139.
(3) Becker, O.; Cheng, Y.; Varley, J. R.; Simon, G. P. *Macromolecules* **2003**, *36*, 1616−1625.
(4) Alexandre, M.; Dubois, P. *Mater. Sci. Eng.* **2000**, *28*, 1−63.
(5) Pinnavaia, T. J., Beall, G. W., Eds. *Polymer-Layered Silicate Nanocomposites*; John Wiley & Sons Ltd.: New York, 2001.
(6) Osborn, K. R.; Jenkins, W. A. *Plastic Films*: *Technology and Packaging Applications*; Technomic Publishing Company, Inc.: Lancaster, PA, 1992.
(7) LeBaron, P. C.; Wang, Z.; Pinnavaia, T. J. *Appl. Clay Sci.* **1999**; *15*, 11−29.
(8) Maiti, P.; Okamoto, M. *Macromol. Mater. Eng.* **2003**, *288*, 440−445.
(9) Hoffmann, B.; Kressler, J.; Stoppelmann, G.; Friedrich, C.; Kim, G. M. *Colloid Polym. Sci.* **2000**, *278*, 629−636.
(10) Matayabas, J. R. *J. C. in Proceedings of NovaPack Europe '99*; September, 1999; p 23.
(11) Harada, M. *Plast. Eng.* **1988**, *44* (1), 27.
(12) Cho, J. W.; Paul, D. R. *Polymer* **2001**, *42*, 1083−1094.
(13) Fornes, T. D.; Yoon, P. J.; Keskkula, H.; Paul, D. R. *Polymer* **2001**, *42*, 9929−9940.

(14) Bharadwaj, R. K. *Macromolecules* **2001**, *34*, 9189−9192.
(15) Fornes, T. D.; Paul, D. R. *Polymer* **2003**, *44*, 4993−5013.
(16) Maiti, P.; Okamoto, M. *Macromol. Mater. Eng.* **2003**, *288*, 440−445.
(17) La Mantia, E. P.; Lo Verso, S.; Tzankova Dintcheva, N. *Macromol. Mater. Eng.* **2002**, *12*, 909−914.
(18) Hu, Y.; Wang, S.; Ling, Z.; Zhuang, Y.; Chen, Z.; Fan, W. *Macromol. Mater. Eng.* **2003**, *288*, 272−276.
(19) Liu, L.; Qi, Z.; Zhu, X. *J. Appl. Polym. Sci.* **1999**, *71*, 1133.
(20) Liu, X.; Wu, Q. *Macromol. Mater. Eng.* **2002**, *287*, 180−186.
(21) Incarnato, L.; Scarfato, P.; Russo, G. M.; Di Maio, L.; Iannelli, P.; Acierno, D. *Polymer* **2003**, *44*, 4625−4643.
(22) Incarnato, L.; Scarfato, P.; Scatteia, L.; Acierno, D. *Polymer* **2004**, *45*, 3487−3496.
(23) Khanna, Y. P.; Han, P. K. *Polym. Eng. Sci.* **1996**, *36*, 1745.
(24) Krishnamoorti, R.; Vaia, R. A.; Giannelis, E. P. *Chem. Mater.* **1996**, *8*, 107.
(25) Fornes, T. D.; Paul, D. R. *Polymer* **2001**, *44*, 1993.
(26) Wagener, R.; Reisinger, T. J. G. *Polymer* **2003**, *44*, 7513−7518.
(27) Bicerano, J. *Prediction of Polymer Properties*, 2nd ed.; Marcel Dekker: New York, 1996.
(28) Krishnamoorti, R.; Vaia, R. A.; Giannelis, E. P. *Chem. Mater.* **1996**, *8*, 1728−1734.
(29) Wu, Z.; Zhou, C.; Zhou, N. *Polym. Testing* **2002**, *21*, 479−483.
(30) Liu, X.; Wu, Q.; Berglund, L. A.; Qi, Z. *Macromol. Mater. Eng.* **2002**, *287*, 515−522.
(31) Liu, X.; Wu, Q. *Polymer* **2002**, *43*, 1933−1936.
(32) Kyotani, M.; Mitsuhashi, S. J. *Polym. Sci Part A-2* **1972**, *10*, 1497−1508.
(33) Fornes, T. D.; Paul, D. R. *Polymer* **2003**, *44*, 3945−3961.
(34) Comyn, J. editor. *Polymer Permeability*, Elsevier Appl. Sci. Publ. Ltd.: New York, 1988.
(35) Nielsen, L. E. *J. Macromol. Sci. Chem.* **1967**, *A1*, 929.

MA052178H